



Comparison of UV/H₂O₂, UV/PMS, and UV/PDS in Destruction of Different Reactivity Compounds and Formation of Bromate and Chlorate

Ying-Hong Guan*, Jin Chen, Li-Jun Chen, Xin-Xin Jiang and Qiang Fu*

School of Water Conservancy and Civil Engineering, Northeast Agricultural University, Harbin, China

OPEN ACCESS

Edited by:

Liangliang Wei,
Harbin Institute of Technology, China

Reviewed by:

Zhengqian Liu,
Huazhong University of Science and
Technology, China
Pengchao Xie,
Huazhong University of Science and
Technology, China
Jingyun Fang,
Sun Yat-sen University, China

*Correspondence:

Ying-Hong Guan
guanyinghong@neau.edu.cn
Qiang Fu
fuqiang@neau.edu.cn

Specialty section:

This article was submitted to
Green and Sustainable Chemistry,
a section of the journal
Frontiers in Chemistry

Received: 08 July 2020

Accepted: 18 August 2020

Published: 25 September 2020

Citation:

Guan Y-H, Chen J, Chen L-J,
Jiang X-X and Fu Q (2020)
Comparison of UV/H₂O₂, UV/PMS,
and UV/PDS in Destruction of
Different Reactivity Compounds and
Formation of Bromate and Chlorate.
Front. Chem. 8:581198.
doi: 10.3389/fchem.2020.581198

In this study, we compared the decontamination kinetics of various target compounds and the oxidation by-products (bromate and chlorate) of PMS, PDS, and H₂O₂ under UV irradiation (UV/PMS, UV/PDS, UV/H₂O₂). Probes of different reactivity with hydroxyl and sulfate radicals, such as benzoic acid (BA), nitrobenzene (NB), and trichloromethane (TCM), were selected to compare the decontamination efficiency of the three oxidation systems. Experiments were performed under acidic, neutral, and alkaline pH conditions to obtain a full-scale comparison of UV/peroxides. Furthermore, the decontamination efficiency was also compared in the presence of common radical scavengers in water bodies [bicarbonate, carbonate, and natural organic matter (NOM)]. Finally, the formation of oxidation by-products, bromate, and chlorate, was also monitored in comparison in pure water and tap water. Results showed that UV/H₂O₂ showed higher decontamination efficiency than UV/PDS and UV/PMS for BA degradation while UV/H₂O₂ and UV/PMS showed better decontamination performance than UV/PDS for NB degradation under acidic and neutral conditions. UV/PMS was the most efficient among the three processes for BA and NB degradation under alkaline conditions, while UV/PDS was the most efficient for TCM degradation under all pH conditions. In pure water, both bromate and chlorate were formed in UV/PDS, small amounts of bromate and rare chlorate were observed in UV/PMS, and no detectable bromate and chlorate were formed in UV/H₂O₂. In tap water, no bromate and chlorate were detectable for all three systems.

Keywords: UV/H₂O₂, UV/persulfate, UV/peroxymonosulfate, bromate, chlorate

INTRODUCTION

Sulfate radical (SO₄⁻)-based advanced oxidation process has attracted increasing attention as an alternative for traditional hydroxyl radical (HO[·])-based advanced oxidation process, due to its high oxidation ability (redox potential of 2.5–3.1 V) (Neta et al., 1988) and adjustability to generating HO[·] via pH manipulation (Guan et al., 2011). SO₄⁻ was generated through activation of peroxymonosulfate (PMS) and peroxydisulfate (PDS) by UV irradiation, electrolysis, base, heat, quinones, ozone, homogeneous, and heterogeneous transition metals (Anipsitakis and Dionysiou, 2004; Furman et al., 2010; Guan et al., 2013; Cong et al., 2015; Zrinyi and Pham, 2017; Chi et al., 2019; Ding et al., 2020; Li et al., 2020; Liu et al., 2020).

PMS, PDS, and hydrogen peroxide (H_2O_2) all have similar -O-O- bond and were usually investigated in comparison. A comparison of UV/PDS and UV/ H_2O_2 was made on decontamination efficiencies. UV/PDS showed a better performance than UV/ H_2O_2 on the removal of carbamazepine (CBZ), 2,4-bromophenol, ofloxacin (OFX), ibuprofen, and cylindrospermopsin (CYN) (He et al., 2013; Yang et al., 2017; Sun et al., 2019; Luo et al., 2019; Xiao et al., 2020a). In studying the degradation of beta amide antibiotics, TOC removal by UV/PDS was slightly better than that by UV/ H_2O_2 (He et al., 2014). The better performance of UV/PDS on decontamination than UV/ H_2O_2 was mainly ascribed to two factors: (1) the higher quantum yield of PDS ($\Phi = 0.7 \text{ mol Einstein}^{-1}$) than that of H_2O_2 ($\Phi = 0.5 \text{ mol Einstein}^{-1}$) and (2) lower steady-state concentration of $\text{HO}\cdot$ than $\text{SO}_4^{\cdot-}$ (Yang et al., 2017). The comparison of three UV/peroxide processes (UV/PMS, UV/PDS, and UV/ H_2O_2) was carried out on destruction of atrazine (ATZ), and it was found that the degradation of UV/PDS on ATZ was more efficient than that of UV/PMS and UV/ H_2O_2 under the same conditions. It was attributed to the fact that the molar extinction coefficient and quantum efficiency of PDS at 254 nm are higher than those of UV/ H_2O_2 and UV/PMS (Luo et al., 2015). However, UV/ H_2O_2 exhibited better performance than UV/PDS on clonidine (CLD) removal that initial degradation rate of CLD was 0.68 and $0.46 \mu\text{M min}^{-1}$ for UV/ H_2O_2 and UV/PDS. The removal efficiencies were 86.5 and 78.7% in UV/ H_2O_2 and UV/PS by the end of experiments, respectively (Xiao et al., 2020b). When removing imidacloprid, UV/PDS showed higher removal efficiency than UV/PMS. This phenomenon was explained by calculating the rate of radical generation and the radical generation rate of UV/PS is higher than that of UV/PMS (Wang Q. F. et al., 2020), while for the removal of tetracycline, degradation efficiency in UV/PMS was higher than that in UV/PDS (Hu et al., 2019). For the three UV/peroxide processes, the superior process varied as target compound changed. The reactivity of target compound would make a sound besides molar extinction coefficient and quantum efficiency. The comparison of UV/peroxide processes need to be performed on target compounds with different reactivity.

When Br^- - or Cl^- -containing water was treated by advanced oxidation process, $\text{HO}\cdot$ and $\text{SO}_4^{\cdot-}$ could react with them to form $\text{Br}\cdot$ or $\text{Cl}\cdot$. $\text{Br}\cdot$ or $\text{Cl}\cdot$ could react with Br^- or Cl^- to form $\text{Br}_2^{\cdot-}$ or $\text{Cl}_2^{\cdot-}$. HOBr/BrO^- or HOCl/ClO^- was formed by $\text{Br}\cdot/\text{Br}_2^{\cdot-}$ or $\text{Cl}\cdot/\text{Cl}_2^{\cdot-}$ recombination. HOBr/BrO^- was reported to be a requisite intermediate in BrO_3^- formation via pure $\text{HO}\cdot$ mechanism (von Gunten and Oliveras, 1998). In UV/PDS, BrO_3^- was formed significantly in the presence of Br^- . HOBr/BrO^- was also thought as a requisite intermediate in UV/PDS. Br^- was initially oxidized by $\text{SO}_4^{\cdot-}$ to form HOBr/BrO^- and the intermediate HOBr/BrO^- was then oxidized by $\text{SO}_4^{\cdot-}$ or photolysis to BrO_3^- (Fang and Shang, 2012). Addition of organic matters could suppress BrO_3^- formation by scavenging $\text{Br}\cdot$ (Liu et al., 2018; Wang Z. Y. et al., 2020). BrO_3^- was formed during oxidation of 2,4-bromophenol by UV/PDS while BrO_3^- was not formed in UV/ H_2O_2 (Luo et al., 2019). BrO_3^- was also formed in UV/PMS and a yield of BrO_3^- reached 100% at

PMS concentration of $500 \mu\text{M}$ (Luo et al., 2020). A substantial conversion of Cl^- into ClO_3^- was observed in UV/PDS at pH 3 and no ClO_3^- was observed at pH >5. It was proposed that $\text{Cl}\cdot$ formed from the reaction between $\text{SO}_4^{\cdot-}$ and Cl^- , initiated a cascade of subsequent pH-dependent reactions to form ClO_3^- (Lutze et al., 2015). In the process of oxidation, $\text{SO}_4^{\cdot-}$ was the main reaction species, and all chloride chain reactions were initiated by $\text{SO}_4^{\cdot-}$ (Qian et al., 2016). HOCl/ClO^- was observed as an intermediate during the formation of ClO_3^- in UV/PDS (Hou et al., 2018), while there was no study referring to the formation of ClO_3^- in UV/PMS process. The comparison of BrO_3^- and ClO_3^- formation in the three UV/peroxide processes was also rarely reported.

The objective of this study was to compare (i) decontamination efficiencies of UV/peroxide processes (UV/PMS, UV/PDS, and UV/ H_2O_2) under various conditions and (ii) the formation of bromate and chlorate experimentally. Benzoic acid (BA), a recalcitrant organic compound, is mainly used in the food and pharmaceutical industries (Rayaroth et al., 2017). It has high reaction rate constants with both $\text{HO}\cdot$ and $\text{SO}_4^{\cdot-}$. Thus, BA was used as a probe to indicate the total oxidation capacity of available $\text{HO}\cdot$ and $\text{SO}_4^{\cdot-}$ (Guan et al., 2011). Nitrobenzene (NB), a refractory pollutant, was used in chemical industry and released into the environment with the amount of about 19 million pounds each year through use, leakage, or industrial accidents (Wei et al., 2019). NB was selected as an indicator for $\text{HO}\cdot$ since it has high rate constant with $\text{HO}\cdot$ but quite low reaction rate constant with $\text{SO}_4^{\cdot-}$ (Guan et al., 2011). Trichloromethane (TCM), a kind of disinfection by-product, has low rate constant with $\text{HO}\cdot$ and $\text{SO}_4^{\cdot-}$ (Guan et al., 2018) and was used as representative of low reactivity organic pollutant. Firstly, total oxidation capacity of available $\text{HO}\cdot$ and $\text{SO}_4^{\cdot-}$ in UV/peroxide processes and the inhibition of common radical scavengers [bicarbonate, carbonate, and natural organic matter (NOM)] on the UV/peroxide processes were investigated with BA as probe. Then, decontamination efficiencies were compared among UV/peroxides with BA, NB, and TCM as probes to present the performance of UV/peroxide processes on removal of different reactivity organic pollutants under various typical pH values. Finally, the formation of bromate and chlorate in pure water and tap water was monitored. The results would provide comprehensive comparison of UV/peroxide processes and guideline for selection of advanced oxidation process constructed based on UV disinfection unit.

MATERIALS AND METHODS

Materials

Potassium peroxymonosulfate (PMS), potassium peroxodisulfate (PDS), BA, NB, sodium phosphate dibasic, sodium phosphate monobasic, sodium chloride, and potassium bromide were all ACS reagent grade and purchased from Sigma-Aldrich Company. Bromate standard for IC and chlorate standard for IC were also from Sigma-Aldrich Company. Hydrogen peroxide solution (35% w/w) was purchased from Alfa Aesar. HPLC

grade phosphoric acid and methanol are available from DIMA-Tech and Thermo Fisher Science Inc. Gas chromatography (GC) grade chloroform (TCM) was purchased from Tianjin Chemical Reagent Co., Ltd. Suwannee River NOM (1R101N) was obtained from the International Humus Society, and the other reagents were of analytical reagent grade and purchased from China National Pharmaceutical Chemical Reagent Co., Ltd. All solutions were prepared in Milli-Q water (18.2 MΩ cm) produced by Milli-Q Biocel water system.

Experimental Procedures

All the photochemical experiments were carried out in a cylindrical borosilicate glass container with a low-pressure mercury UV lamp (Heraeus, GPH 135t5l/4, 6 W output, 254 nm). The incident radiation intensities of the UV lamp (I_0) were 1.7×10^{-6} Einstein s^{-1} (0.6 L solution) and 1.92×10^{-6} Einstein s^{-1} (0.55 L solution). The optical path lengths (L) of the two reactor vessels were 2.70 cm (0.6 L solution) and 2.63 cm (0.55 L solution), respectively. Samples were extracted at predetermined intervals for each experiment and quenched with excess ascorbic acid or sodium nitrite. In the cases of tests in tap water, bromide was added to monitor the formation of bromate while no additional chloride was added for monitoring chlorate formation. Water quality parameters of tap water are shown in **Table 5**. All experiments were carried out at room temperature ($20 \pm 2^\circ\text{C}$). The error bar represents the standard deviation of repeated experiments.

Analytical Methods

The concentrations of BA and NB were determined by high-performance liquid chromatography (HPLC) equipped with Waters 2,487 double λ detector and Waters symbol C18 column (4.6 mm \times 150 mm, particle size 5 μm). TCM was quantified by gas chromatography (Agilent GC 6890). Details could be found in previous studies (Guan et al., 2011, 2018). Concentrations of anions (chloride, bromide, chlorate, and bromate) were analyzed using a high-pressure ion chromatograph (Dionex Integriion) equipped with a Dionex AS19 column (4 \times 250 mm). Isocratic eluent of 20 mM KOH, generated online by Dionex EGC 500 KOH, was used to separate the anions at the rate of 1.0 ml min^{-1} with a suppressor current of 50 mA. The injection volume was 200 μl and detection limits for bromate and chlorate were 0.01 and 0.01 μM . PMS concentration was standardized by iodometric titration (Ball et al., 1967). H_2O_2 concentration was standardized based on its absorbance at 240 nm ($\epsilon = 40 \text{ M}^{-1}\cdot\text{cm}^{-1}$) (Bader et al., 1988) and PDS concentration was quantified at 254 nm ($\epsilon = 20 \text{ M}^{-1}\cdot\text{cm}^{-1}$) (Zhang et al., 2018). Pseudo-first-order rate constant (k_0) of target compound degradation was obtained by fitting data of removal efficiency within 75%.

In some cases, such as UV/PMS and UV/ H_2O_2 processes at pH 11, the decontamination process could not be well-fitted by first-order reaction kinetics. Herein, we introduced the relative difference of removal efficiency (RDRE) of UV/peroxide processes to depict the inhibition effect of inorganic and organic carbon on

UV/peroxide processes, which was calculated based on Equation (1).

$$RDRE = \frac{1}{n} \times \sum_{i=1}^n \frac{(c_i/c_0 - c_i'/c_0')}{1 - c_i/c_0} \quad (1)$$

where i is the index of sampling times ranging from 1 to n , n is the sample number. c_i is the concentration of BA at sample time i in the absence of bicarbonate, carbonate, or NOM. c_i' is the concentration of BA at the same sample time i in the presence of bicarbonate, carbonate, or NOM. c_0 is the initial concentration of BA in the absence of bicarbonate, carbonate, or NOM, and c_0' is the initial concentration of BA in the presence of bicarbonate, carbonate, or NOM. Positive values of RDRE indicate the stimulation of additive, and negative values indicate the inhibition of additive. The larger the absolute value is, the stronger the stimulation or inhibition effect is.

RESULTS AND DISCUSSION

Decontamination in the Presence of Common Radical Scavengers

Inorganic carbon (HCO_3^- and CO_3^{2-}) and NOM are widely present in surface water and groundwater, and regarded as free radical scavengers, leading to weakening the oxidation of target organic pollutants by advanced oxidation processes (Benndesen et al., 2012). $\text{HO}\cdot$ and $\text{SO}_4^{\cdot-}$ have different reactivity with inorganic and organic carbon, and the difference of reactivity would lead to a different effect on decontamination efficiency in $\text{HO}\cdot$ and $\text{SO}_4^{\cdot-}$ -based oxidation process. BA was used as a probe

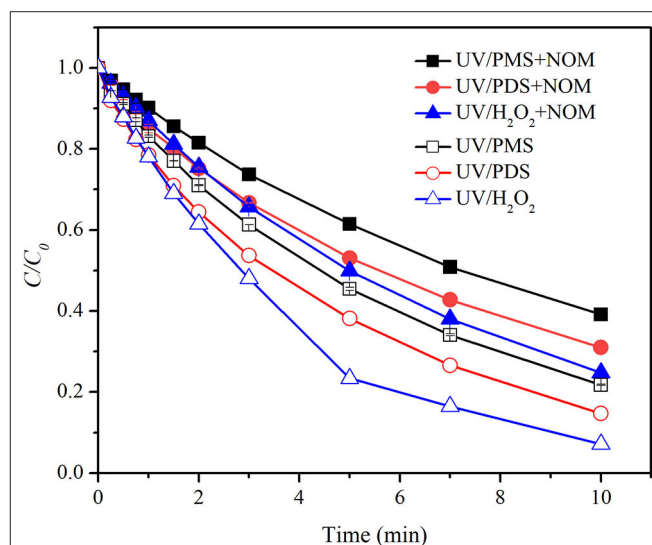


FIGURE 1 | Degradation efficiencies of BA by UV/PMS, UV/PDS, and UV/ H_2O_2 in the presence of NOM. Conditions: 0.6 L, $I_0 = 1.7 \times 10^{-6}$ Einstein s^{-1} , $[\text{P}^{\cdot-}] = 2 \text{ mM}$, $[\text{BA}] = 9.0 \mu\text{M}$, $[\text{PMS}] = 100 \mu\text{M}$ as 1/2 Oxone, $[\text{H}_2\text{O}_2] = 100 \mu\text{M}$, $[\text{PDS}] = 100 \mu\text{M}$, $[\text{NOM}] = 2.23 \text{ mgTOC}\cdot\text{L}^{-1}$, pH = 7.0 \pm 0.1, 25°C.

TABLE 1 | Pseudo-first-order rate constant (k_0) of BA degradation in the presence and absence of radical scavengers in UV/peroxides obtained by fitting data of BA removal within 75%.

UV/peroxide processes	pH 7		pH 7, NOM		pH 8		pH 8, bicarbonate		pH 11		pH 11, carbonate	
	k_0 (s ⁻¹)	R^2 of linear fit	k_0' (s ⁻¹)	R^2 of linear fit	k_0 (s ⁻¹)	R^2 of linear fit	k_0' (s ⁻¹)	R^2 of linear fit	k_0 (s ⁻¹)	R^2 of linear fit	k_0' (s ⁻¹)	R^2 of linear fit
UV/PMS	0.00263	0.99815	0.00160	0.99913	0.00302	0.99785	0.00135	0.99881	0.01231	0.99303	0.00106	0.97997
UV/PDS	0.00326	0.99996	0.00203	0.99629	0.00321	0.99495	0.00107	0.99924	0.00451	0.99917	0.00036	0.99717
UV/H ₂ O ₂	0.00454	0.99248	0.00232	0.99996	0.00409	0.99924	0.00164	0.99656	0.00392	0.99911	0.00046	0.95388

TABLE 2 | Relative differences of k_0 between UV/peroxide processes and UV/peroxide processes in the presence of additives (radical scavengers) (k_0'/k_0).

UV/peroxide processes	NOM	Bicarbonate	Carbonate
UV/PMS	-0.3916	-0.5530	-0.9139
UV/PDS	-0.3773	-0.6667	-0.9202
UV/H ₂ O ₂	-0.4890	-0.5990	-0.8827

TABLE 3 | Relative differences of removal efficiencies (RDRE) between UV/peroxide processes and UV/peroxide processes in the presence of additives (radical scavengers).

UV/peroxide processes	NOM	Bicarbonate	Carbonate
UV/PMS	-0.3468	-0.5008	-0.7878
UV/PDS	-0.3069	-0.6279	-0.8886
UV/H ₂ O ₂	-0.3632	-0.4466	-0.7507

for both HO· and SO₄⁻ to compare the total oxidation capacity and further investigate the influence of inorganic and organic carbon on total oxidation capacity of the three processes.

As shown in **Figure 1**, BA degradation in UV/H₂O₂ and UV/PDS was faster than that in UV/PMS under neutral conditions (pH 7). The presence of 2.23 mgTOC·L⁻¹ NOM showed inhibition on BA degradation in all the systems. Pseudo-first-order rate constant (k_0) of BA degradation was obtained by fitting data of BA removal within 75% and shown in **Table 1**. k_0 of BA degradation was 0.00263, 0.00326, and 0.00454 s⁻¹ in UV/PMS, UV/PDS, and UV/H₂O₂ at pH 7. By adding NOM, values of k_0 were reduced to 0.00160, 0.00203, and 0.00232 s⁻¹ in UV/PMS, UV/PDS, and UV/H₂O₂, respectively. BA degradation appeared to be still the fastest in UV/H₂O₂ after addition of NOM. The presence of NOM led to the relative decrease of k_0 of 39.16, 37.73, and 48.90% in UV/PMS, UV/PDS, and UV/H₂O₂, respectively, as shown in **Table 2**. The values of RDRE between UV/peroxide processes and UV/peroxide processes in the presence of NOM were -0.3468, -0.3069, and -0.3632 in UV/PMS, UV/PDS, and UV/H₂O₂ (**Table 3**). The two indexes, reflecting NOM effect on decontamination, both indicated that NOM showed the largest inhibition on UV/H₂O₂ process and the smallest on UV/PDS process. Although HO·

has a higher reactivity with BA (5.9×10^9 M⁻¹·s⁻¹) than SO₄⁻ (1.2×10^9 M⁻¹·s⁻¹), it also has a higher rate constant with NOM [1.4×10^4 (mgTOC·L⁻¹)⁻¹·s⁻¹] than SO₄⁻ [2.2×10^3 (mgTOC·L⁻¹)M⁻¹·s⁻¹] (Reactions 2 and 3) (Guan et al., 2018). The value of $k_{\text{radical,BA}}/k_{\text{radical,NOM}}$ for HO· (ratio of rate constant of HO· and BA to that of HO· and NOM, 4.21×10^5 mgTOC·L⁻¹·M⁻¹) was smaller than that for SO₄⁻ (5.45×10^5 mgTOC·L⁻¹·M⁻¹), which resulted in a slight higher inhibition of NOM on HO· than SO₄⁻. This led to the larger inhibition of NOM on the UV/H₂O₂ process and less on the UV/PDS process.



$$k = 1.4 \times 10^4 (\text{mgTOC} \cdot \text{L}^{-1})^{-1} \text{s}^{-1} \quad (2)$$



$$k = 2.2 \times 10^3 (\text{mgTOC} \cdot \text{L}^{-1})^{-1} \text{s}^{-1} \quad (3)$$

Figure 2 shows the effect of bicarbonate on BA degradation in UV/peroxides. k_0 values of BA degradation were 0.00302, 0.00321, and 0.00409 s⁻¹ in UV/PMS, UV/PDS, and UV/H₂O₂ at pH 8. k_0 values were decreased to 0.00135, 0.00107, and 0.00164 s⁻¹ in UV/PMS, UV/PDS, and UV/H₂O₂ by adding bicarbonate (**Table 1**). UV/H₂O₂ was still the most efficient process in the presence of bicarbonate for BA degradation. **Figure 3** shows the effect of carbonate on BA degradation in UV/peroxides. k_0 values of BA degradation at pH 11 were 0.01231, 0.00451, and 0.00392 s⁻¹ in UV/PMS, UV/PDS, and UV/H₂O₂, while k_0 values in the presence of carbonate were 0.00106, 0.00036, and 0.00046 s⁻¹ in UV/PMS, UV/PDS, and UV/H₂O₂ (**Table 1**). Carbonate showed significant inhibition on decontamination in all the UV/peroxide processes. In the presence of carbonate, UV/PMS was the most efficient process for BA degradation. This was due to the larger quantity of HO· and SO₄⁻ produced by PMS photolysis since PMS has a quite large molar absorbance coefficient (146.4 M⁻¹ cm⁻¹) at pH 11 (Guan et al., 2011). Relative decrease of k_0 and RDRE caused by the addition of bicarbonate and carbonate (as shown in **Tables 2, 3**) indicated that bicarbonate and carbonate showed the largest inhibition on the UV/PDS process. Furthermore, carbonate showed larger inhibition on UV/peroxide processes than bicarbonate, while the difference of bicarbonate inhibition extent among UV/peroxide processes was more obvious than carbonate.

The rate constants of HO· and SO₄⁻ with bicarbonate were 8.5×10^6 M⁻¹·s⁻¹ and 3.6×10^6 M⁻¹·s⁻¹ (Reactions 4 and

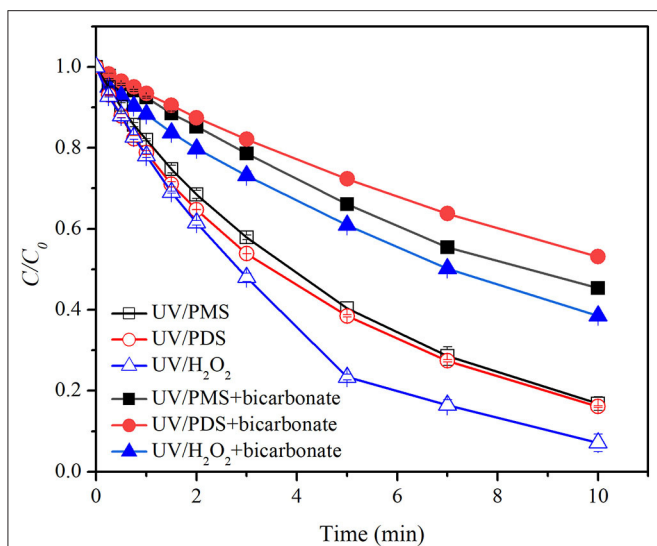


FIGURE 2 | Degradation efficiencies of BA by UV/PMS, UV/PDS, and UV/H₂O₂ in the presence of bicarbonate. Conditions: 0.6 L, $I_0 = 1.7 \times 10^{-6}$ Einsteins·s⁻¹, [PB] = 2 mM, [BA] = 9.0 μM, [PMS] = 100 μM as 1/2 Oxone, [H₂O₂] = 100 μM, [PDS] = 100 μM, [HCO₃⁻] = 10 mM, pH = 8.0 ± 0.1, 25°C.

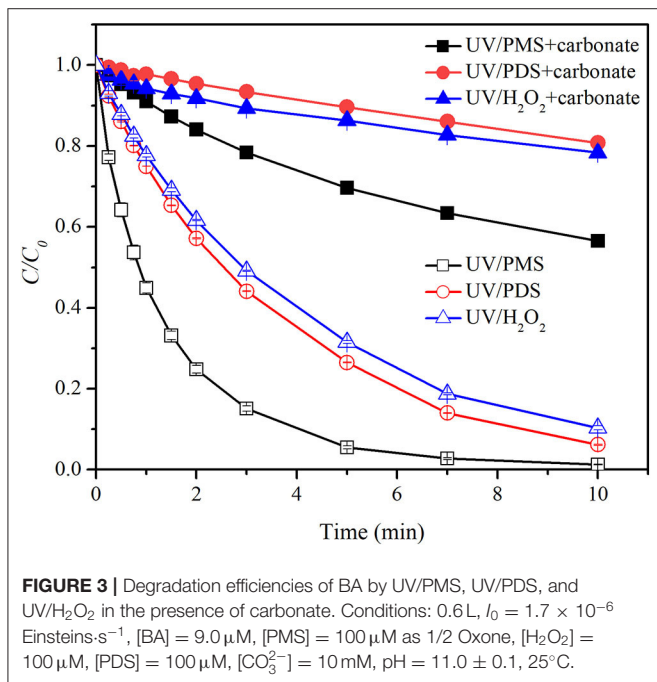
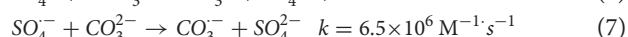
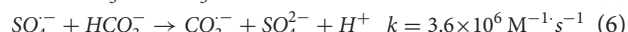
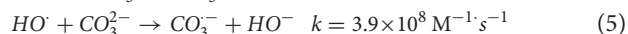
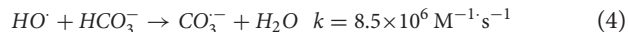


FIGURE 3 | Degradation efficiencies of BA by UV/PMS, UV/PDS, and UV/H₂O₂ in the presence of carbonate. Conditions: 0.6 L, $I_0 = 1.7 \times 10^{-6}$ Einsteins·s⁻¹, [BA] = 9.0 μM, [PMS] = 100 μM as 1/2 Oxone, [H₂O₂] = 100 μM, [PDS] = 100 μM, [CO₃²⁻] = 10 mM, pH = 11.0 ± 0.1, 25°C.

6) (Zhang et al., 2018). The values of $k_{\text{radical,BA}}/k_{\text{radical,bicarbonate}}$ (ratio of rate constant of radical and BA to that of radical and bicarbonate) for HO· and SO₄⁻ were calculated to be 6.94×10^2 and 3.33×10^2 , respectively. As a result, bicarbonate showed a slightly higher inhibition on SO₄⁻ than HO· and correspondingly a larger inhibition on the UV/PDS process. The rate constants of HO· and SO₄⁻ with carbonate were $3.9 \times 10^8 \text{ M}^{-1}\cdot\text{s}^{-1}$ and $6.5 \times 10^6 \text{ M}^{-1}\cdot\text{s}^{-1}$ (Reactions 5 and 7) (Zhang et al., 2018). The values of $k_{\text{radical,BA}}/k_{\text{radical,carboante}}$ (ratio of rate constant of radical and

BA to that of radical and carbonate) for HO· and SO₄⁻ were calculated to be 1.51×10^1 and 1.84×10^2 , respectively. As a result, carbonate would show a higher inhibition on HO· than SO₄⁻. Under alkaline conditions (pH 11), majority of SO₄⁻ was converted into HO·. Therefore, carbonate exhibited significant inhibition on the three processes and the difference of inhibition extent for UV/peroxides was not as much as bicarbonate.



Destruction of Different Organic Target Compounds

Figure 4 shows the comparison of BA degradation by UV/peroxides. k_0 of BA degradation was obtained by fitting data of BA removal within 75% and shown in **Table 4**. k_0 values of BA degradation by UV/PMS under acidic (pH 3), neutral (pH 7), and alkaline conditions (pH 11) were 0.00279, 0.00281, and 0.01244 s⁻¹ at the oxidant concentration of 100 μM. Under the same conditions, the values of k_0 in UV/PDS were 0.00293, 0.00334, and 0.00466 s⁻¹, while k_0 values in UV/H₂O₂ were 0.00435, 0.00434, and 0.00420 s⁻¹ at pH 3, pH 7, and pH 11, respectively. UV/H₂O₂ showed higher decontamination efficiencies than UV/PDS and UV/PMS for BA degradation under acidic and neutral conditions, while UV/PMS showed outstanding decontamination efficiency for BA degradation under alkaline conditions. This indicated that UV/H₂O₂ has a highest total oxidation capacity of available HO· and SO₄⁻ under acidic and neutral conditions while UV/PMS did under alkaline condition. The results were similar to the reported comparison of clonidine (CLD) removal by UV/H₂O₂ and PDS that UV/H₂O₂ exhibited better performance than UV/PDS (Xiao et al., 2020b). It was different from the removal of carbamazepine (CBZ), 2,4-bromophenol, ofloxacin (OFX), ibuprofen, and cyindrospermopsin (CYN) by UV/H₂O₂ and UV/PDS that UV/PDS showed a better performance than UV/H₂O₂ (He et al., 2013; Yang et al., 2017; Luo et al., 2019; Sun et al., 2019; Xiao et al., 2020a). Production rates of radicals from UV/peroxide processes mainly depend on molar extinction coefficients and photolysis quantum yields of peroxides. Molar extinction coefficients of H₂O₂ and its dissociated form HO₂⁻ were 19.6 and 229 M⁻¹·cm⁻¹ (Baxendale and Wilson, 1957) while quantum yield of H₂O₂ photolysis at 254 nm was $\Phi = 0.5$ (Crittenden et al., 1999). Molar extinction coefficients of HSO₅⁻ (monovalent form of PMS) and SO₅²⁻ (divalent form of PMS) were 13.8 and 149.5 M⁻¹·cm⁻¹ while quantum yield of PMS photolysis at 254 nm was $\Phi = 0.52$ (Guan et al., 2011). Molar extinction coefficient and photolysis quantum yield of PDS at 254 nm were reported to be varied in different studies. The values were $\epsilon = 20.07 \text{ M}^{-1}\cdot\text{cm}^{-1}$ and $\Phi = 0.7$ (Zhang et al., 2018), $\epsilon = 22.07 \text{ M}^{-1}\cdot\text{cm}^{-1}$ and $\Phi = 0.5$ (Qian et al., 2016), and $\epsilon = 21.2 \text{ M}^{-1}\cdot\text{cm}^{-1}$ and $\Phi = 0.567$ (Heidt et al., 1948). By considering quantum yield of PDS photolysis

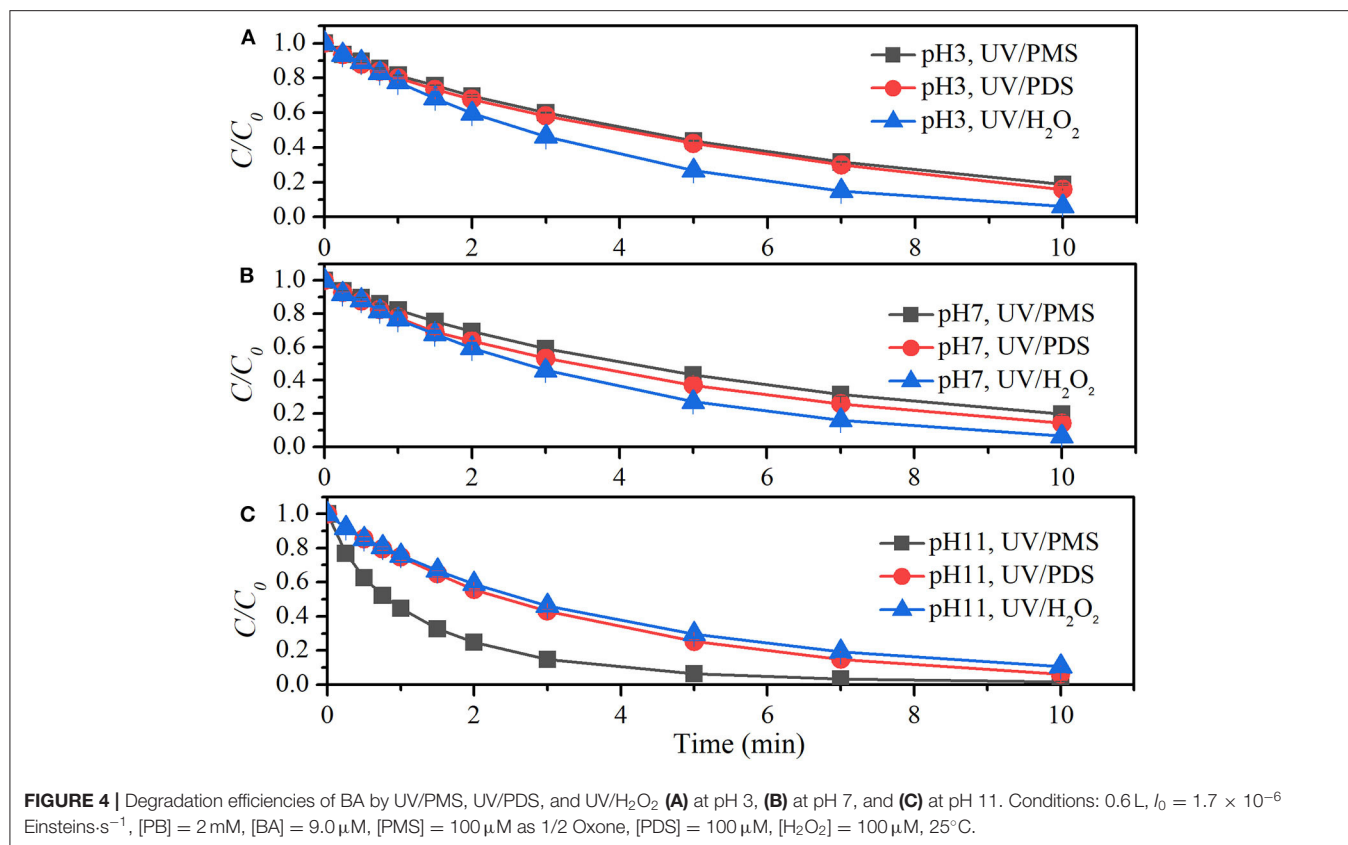


TABLE 4 | Pseudo-first-order rate constant (k_0) of BA, NB, and TCM degradation in UV/peroxide processes under acidic, neutral, and alkaline conditions.

Target compounds	UV/peroxide processes	pH 3		pH 7		pH 11	
		k_0 (s ⁻¹)	R^2 of linear fit	k_0 (s ⁻¹)	R^2 of linear fit	k_0 (s ⁻¹)	R^2 of linear fit
BA	UV/PMS	0.00279	0.99765	0.00281	0.99764	0.01244	0.99134
	UV/PDS	0.00293	0.99569	0.00334	0.99510	0.00466	0.99863
	UV/H ₂ O ₂	0.00435	0.99912	0.00434	0.99924	0.00420	0.99640
NB	UV/PMS	0.00120	0.98997	0.00106	0.97027	0.00483	0.95544
	UV/PDS	0.00107	0.98811	0.00079	0.97768	0.00204	0.97764
	UV/H ₂ O ₂	0.00249	0.99569	0.00204	0.99315	0.00168	0.99028
TCM	UV/PMS	0.00223	0.99713	0.00265	0.99706	0.00117	0.90819
	UV/PDS	0.01524	0.97129	0.01018	0.99438	0.00626	0.99612
	UV/H ₂ O ₂	0.00046	0.96875	0.00039	0.94686	0.00033	0.98305

as $\Phi = 0.5$, the photo-production rates of total radicals at pH 7 from UV/H₂O₂ and UV/PDS were not in big difference, both of which were larger than radical photo-production rate from UV/PMS. This was almost in accordance with the initial degradation of BA at pH 7. With time extension, BA degradation in UV/H₂O₂ appeared strengthened as compared with that in UV/PDS. This might be due to the additional production of HO· via reaction between H₂O₂ and quinones (Koppenol and Butler, 1985), the intermediate product of BA oxidation. As pH decreased from 7 to 3, degradation rate of BA was almost not affected in UV/H₂O₂ and UV/PMS, while degradation rate of BA was slightly slowed down in UV/PDS.

As pH increased from 7 to 11, BA degradation was significantly enhanced in UV/PMS. It was mainly due to the increased photo-production of HO· and SO₄⁻, which originated from the increased molar absorption coefficient from 14.3 to 146.4 M⁻¹·cm⁻¹ (Guan et al., 2011).

Figure 5 and Table 4 show the comparison of UV/peroxide processes on NB degradation. At the oxidant concentration of 100 μM, k_0 values of NB degradation in UV/PMS were 0.00120, 0.00106, and 0.00483 s⁻¹ at pH 3, pH 7, and pH 11, respectively. The values of k_0 in UV/PDS were 0.00107, 0.00079, and 0.00204 s⁻¹ while k_0 values in UV/H₂O₂ were 0.00249, 0.00204, and 0.00168 s⁻¹ at pH 3, pH 7, and pH 11, respectively.

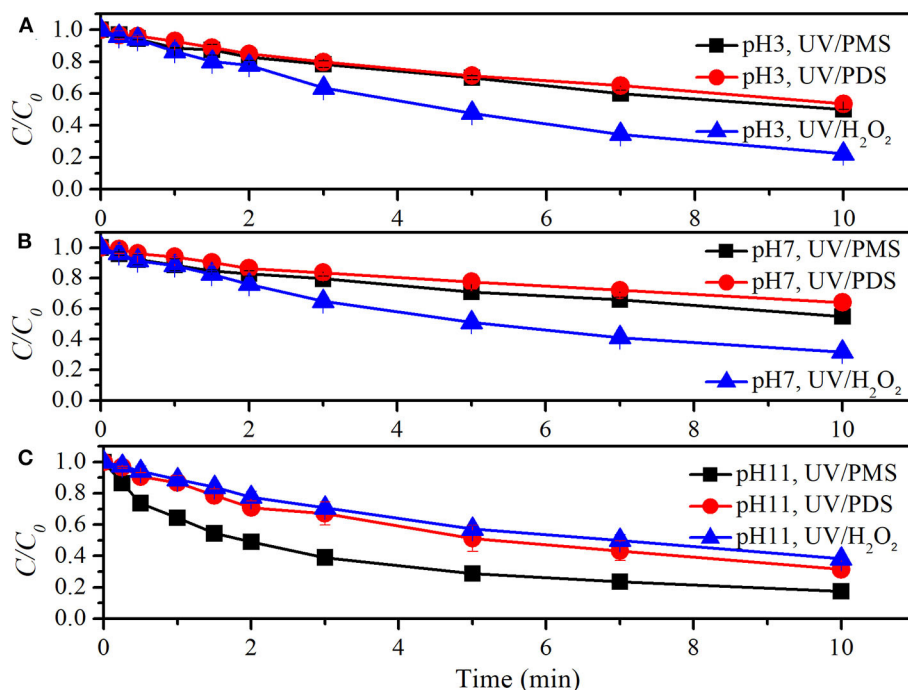


FIGURE 5 | Degradation efficiencies of NB by UV/PMS, UV/PDS, and UV/H₂O₂ (A) at pH 3, (B) at pH 7, and (C) at pH 11. Conditions: 0.6 L, $I_0 = 1.7 \times 10^{-6}$ Einsteins·s⁻¹, [PB] = 2 mM, [NB] = 6.6 μM, [PMS] = 100 μM as 1/2 Oxone, [PDS] = 100 μM, [H₂O₂] = 100 μM, 25°C.

TABLE 5 | Water quality parameters of tap water.

DOC (mg C/L)	Alkalinity (as CaCO ₃ , mg/L)	Cl ⁻ (μM)	Br ⁻ (μM)	NO ₃ ⁻ (μM)	pH
2.78	44.82	535	N.D.	241	6.98

N.D., not detected.

The performance of UV/peroxides declined in the sequence of UV/H₂O₂ > UV/PMS > UV/PDS for NB degradation under acidic and neutral conditions. Meanwhile, UV/PMS also showed excellent decontamination for NB degradation under alkaline conditions. The declined decontamination of UV/H₂O₂ from pH 7 to 11 might be due to the increased capture of HO· by hydrogen peroxide and fast depletion of hydrogen peroxide (Crittenden et al., 1999), although the increase of pH would lead to the increased molar absorption coefficient of hydrogen peroxide (Baxendale and Wilson, 1957), intending to increase photo-production of HO·. The rate constants of PDS with SO₄⁻ and HO· were $6.3 \times 10^5 \text{ M}^{-1}\cdot\text{s}^{-1}$ and $1.4 \times 10^7 \text{ M}^{-1}\cdot\text{s}^{-1}$ (Guan et al., 2018). The rate constants of NB with SO₄⁻ and HO· were $\leq 10^6 \text{ M}^{-1}\cdot\text{s}^{-1}$ and $3.9 \times 10^9 \text{ M}^{-1}\cdot\text{s}^{-1}$ (Guan et al., 2011). The ratios of $k_{\text{radical,NB}}$ (rate constant of radical and NB) to $k_{\text{radical,PDS}}$ (rate constant of radical and PDS) were ≤ 1.6 and 2.8×10^2 for SO₄⁻ and HO·. Correspondingly, the ratios of $k_{\text{radical,NB}}\cdot c_{\text{NB}}$ to $k_{\text{radical,PDS}}\cdot c_{\text{PDS}}$ were ≤ 0.1 and 18.4 for SO₄⁻ and HO· by considering the initial concentrations of NB and PDS. More SO₄⁻ was captured by the parent oxidant

PDS than HO·. The enhanced decontamination of UV/PDS with pH increasing was mainly due to the conversion of SO₄⁻ into HO·, since HO· has a higher radical usage efficiency than SO₄⁻.

Figure 6 and Table 4 show the comparison of TCM degradation by UV/peroxides. UV/H₂O₂ showed limited degradation of TCM that about 30% of TCM was obtained by 15 min under all the investigated pH values at the oxidant concentration of 500 μM. UV/PDS showed excellent performance on TCM removal that more than 95% of TCM was degraded by 15 min under all pH conditions. k_0 values of TCM degradation at pH 3, pH 7, and pH 11 were 0.00223, 0.00265, and 0.00117 s⁻¹ in the UV/PMS process, 0.01524, 0.01018, and 0.00626 s⁻¹ in the UV/PDS process, and 0.00046, 0.00039, and 0.00033 s⁻¹ in the UV/H₂O₂ process, respectively. UV/peroxide performance was in the increased sequence of UV/H₂O₂ < UV/PMS < UV/PDS under all pH conditions. During TCM degradation, Cl⁻ was formed as the final product. Cl· would be generated when Cl⁻ coexisted with SO₄⁻ and/or HO· (Lutze et al., 2015; Guan et al., 2018). The limited removal of TCM by UV/H₂O₂ might be due to the scavenging of radicals (SO₄⁻, HO·, Cl·, and phosphate radical) by hydrogen peroxide, leading to the low efficiency of radicals for TCM degradation in UV/H₂O₂. In UV/PDS, TCM removal decreased as pH increased from 7 to 11. The rate constants of PDS with SO₄⁻, HO·, and Cl· were $6.3 \times 10^5 \text{ M}^{-1}\cdot\text{s}^{-1}$, $1.4 \times 10^7 \text{ M}^{-1}\cdot\text{s}^{-1}$, and $8.8 \times 10^6 \text{ M}^{-1}\cdot\text{s}^{-1}$ (Guan et al., 2018). The rate constants of TCM with SO₄⁻, HO·, and Cl· were $2 \times 10^6 \text{ M}^{-1}\cdot\text{s}^{-1}$, $6.3 \times 10^7 \text{ M}^{-1}\cdot\text{s}^{-1}$, and $6.6 \times 10^7 \text{ M}^{-1}\cdot\text{s}^{-1}$ (Guan et al., 2018). The ratios of $k_{\text{radical,TCM}}$ (rate

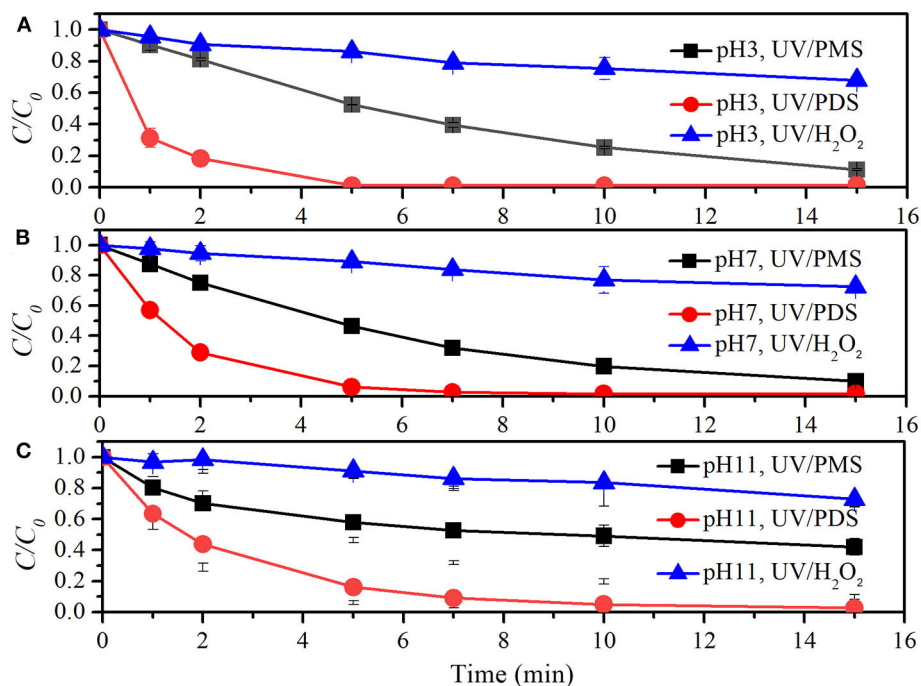


FIGURE 6 | Degradation efficiencies of TCM by UV/PMS, UV/PDS, and UV/H₂O₂ (A) at pH 3, (B) at pH 7, and (C) at pH 11. Conditions: 0.6 L, $I_0 = 1.7 \times 10^{-6}$ Einsteins·s⁻¹, [PB] = 5 mM, [TCM] = 2.1 μM, [PMS] = 0.5 mM as 1/2 Oxone, [PDS] = 0.5 mM, [H₂O₂] = 0.5 mM, 25°C.

constant of radical and TCM) to $k_{\text{radical,PDS}}$ (rate constant of radical and PDS) were 3.2, 4.5, and 7.5 for $\text{SO}_4^{\cdot-}$, HO^{\cdot} , and Cl^{\cdot} , respectively. The ratios reflected the radical efficiency toward TCM against PDS, similar to the radical participation ratio (RPR) reported in UV/PMS (Guan et al., 2018). In the presence of chloride, $\text{SO}_4^{\cdot-}$ was fast converted into Cl^{\cdot} and $\text{Cl}_2^{\cdot-}$ under acidic conditions and increasing pH would lead to conversion of Cl^{\cdot} to HO^{\cdot} (Lutze et al., 2015; Guan et al., 2018). This would lead to the declined TCM degradation as pH increased from 7 to 11. The variation of TCM destruction with pH was similar to the trend of 2-methylisoborneol and geosmin removal vs. pH, which was ascribed to the distribution of phosphate ions (Xie et al., 2015). As pH increased, H_2PO_4^- dissociated to HPO_4^{2-} and HPO_4^{2-} has higher rate constants with HO^{\cdot} and $\text{SO}_4^{\cdot-}$ than H_2PO_4^- . The enhanced scavenging effect of phosphate buffer might also contribute to decrease of TCM removal as pH increased.

The higher removal efficiency for TCM by UV/PDS, as compared with the other two UV/peroxide processes, might be due to the lower scavenging of radicals ($\text{SO}_4^{\cdot-}$, HO^{\cdot} , and Cl^{\cdot}) by the parent oxidant (PDS) in the reaction system. Based on the analysis of removal of BA, NB, and TCM by the UV/peroxide processes, it could be obtained that the decontamination rate would mainly depend on the molar absorption coefficient and radical quantum yield for the target compounds with high rate constants toward both HO^{\cdot} and $\text{SO}_4^{\cdot-}$, while the scavenging effect of the parent oxidant for radicals should also be considered besides molar absorption coefficient and radical quantum yield when choosing the superior process of decontamination rate for the target compounds with low rate constants toward

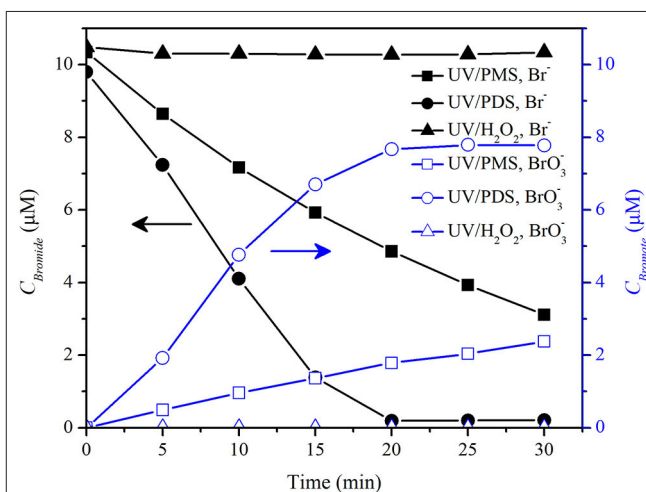


FIGURE 7 | Concentrations of bromide and bromate in UV/PMS, UV/PDS, and UV/H₂O₂. Conditions: [PMS] = 200 μM as 1/2 Oxone, [PDS] = 200 μM, [H₂O₂] = 200 μM, unbuffered, $I_0 = 1.92 \mu\text{Einstein}\cdot\text{s}^{-1}$, $V = 0.55 \text{ L}$, 20°C.

$\text{SO}_4^{\cdot-}$ or toward both HO^{\cdot} and $\text{SO}_4^{\cdot-}$. It would be suggested that UV/PDS might be a good choice for removing chloro-substituted organic compounds with low rate constant with radicals, while UV/PMS was recommended to be used under alkaline conditions and UV/H₂O₂ would be used under acidic and neutral conditions for destructing organic pollutants with high rate constant with radicals.

Bromate and Chlorate Formation

Bromate and chlorate were reported to be formed in UV/PDS in the presence of bromide and chloride (Fang and Shang, 2012; Lutze et al., 2015). However, whether chlorate was formed in the presence of chloride in UV/PMS system was rarely reported. The comparison of bromate and chlorate formation in UV/peroxide processes was also little reported. Hence, bromate and chlorate formation was comparatively investigated in the UV/peroxide systems in pure water and tap water. **Figure 7** shows that BrO_3^- was obviously formed in UV/PDS in pure water background that BrO_3^- concentration was about $7.8 \mu\text{M}$ by 30 min at an initial Br^- concentration of $9.8 \mu\text{M}$ and PDS concentration of $200 \mu\text{M}$, while $2.4 \mu\text{M}$ BrO_3^- was formed in UV/PMS and no BrO_3^- was detected in UV/ H_2O_2 . It was consistent with the results that show that no BrO_3^- was formed during 2,4-bromophenol degradation by UV/ H_2O_2 (Luo et al., 2019).

In UV/PDS, BrO_3^- formation was initiated by the reaction between $\text{SO}_4^{\cdot-}$ and Br^- to form Br^\cdot and subsequent formation of $\text{HOBr}/\text{BrO}^\cdot$. The intermediate $\text{HOBr}/\text{BrO}^\cdot$ was then oxidized by $\text{SO}_4^{\cdot-}$ or photolysis to BrO_3^- (Fang and Shang, 2012). In UV/PMS, Br^\cdot and $\text{Br}_2^{\cdot-}$ formed from Br^- by HO^\cdot and $\text{SO}_4^{\cdot-}$ oxidation via Reactions 8 and 9 might react with PMS, since $\text{Br}^\cdot/\text{Br}_2^{\cdot-}$ (2.0 V) and $\text{Br}_2^{\cdot-}/\text{Br}^-$ (1.63 V) have higher redox potential than $\text{SO}_5^{\cdot-}/\text{HSO}_5^-$ (1.1V) (Ebersson, 1982; Neta et al., 1988). The reaction would slow down or hinder the recombination of $\text{Br}^\cdot/\text{Br}_2^{\cdot-}$ to form $\text{HOBr}/\text{BrO}^\cdot$. However, Br^- could be oxidized by PMS directly via two electron transfer to $\text{HOBr}/\text{BrO}^\cdot$ with a rate constant of $0.7 \text{ M}^{-1} \text{ s}^{-1}$ via Reactions 10 and 11 (Lente et al., 2009; Zhou et al., 2018). About $2 \mu\text{M}$ $\text{HOBr}/\text{BrO}^\cdot$ would form by a rough estimation at a PMS concentration of $200 \mu\text{M}$ and a Br^- concentration of $10 \mu\text{M}$. The above two aspects might be the reasons for the slow formation of BrO_3^- in UV/PMS. H_2O_2 reacted fast with $\text{HOBr}/\text{BrO}^\cdot$ with a second-order rate constant of $1,900 \text{ M}^{-1} \text{ s}^{-1}$ at pH 6 or $1.5 \times 10^4 \text{ M}^{-1} \text{ s}^{-1}$ (Von Gunten and Oliveras, 1997), which would result in the half-life of HOBr of about 1.8 s and 0.2 s at reaction pH 5.7–6.5 with an initial H_2O_2 concentration of $200 \mu\text{M}$. It would lead to complete reduction of HOBr to Br^- . HOBr was a requisite intermediate of bromate (von Gunten and Oliveras, 1998). This resulted in no formation of BrO_3^- in UV/ H_2O_2 as shown in **Figure 7**.

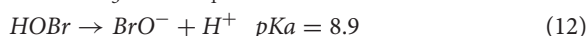
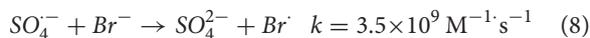
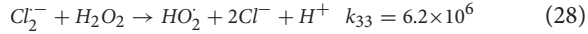
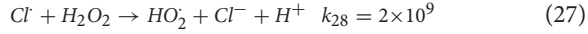
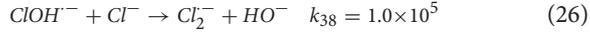
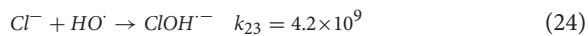
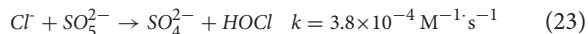
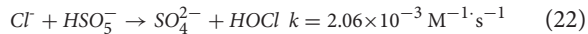
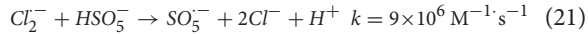
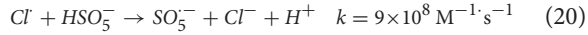
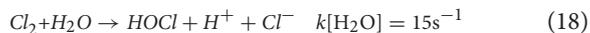
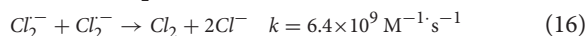
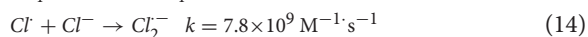
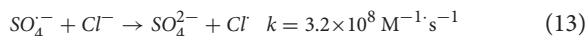


Figure 8 shows the ClO_3^- formation in pure water in the UV/peroxide processes. ClO_3^- was obviously formed in UV/PDS that $4 \mu\text{M}$ ClO_3^- was formed by 30 min in pure water at an initial Cl^- concentration of 0.5 mM and a PDS concentration of $200 \mu\text{M}$. ClO_3^- was slightly formed in UV/PMS that $0.8 \mu\text{M}$ ClO_3^- was formed by 30 min. No ClO_3^- was detected in UV/ H_2O_2 .

Cl^- has a high reaction rate constant with $\text{SO}_4^{\cdot-}$. It would be quickly oxidized by $\text{SO}_4^{\cdot-}$ to form Cl^\cdot and $\text{Cl}_2^{\cdot-}$ (Reactions 13 and 14). In UV/PDS, Cl^\cdot and $\text{Cl}_2^{\cdot-}$ recombine with its self or mutually to yield Cl_2 as Reactions 15–17 (Qian et al., 2016; Guan et al., 2018). Then, Cl_2 hydrolyzes into $\text{HOCl}/\text{ClO}^\cdot$ via Reactions 18 and 19. $\text{HOCl}/\text{ClO}^\cdot$ is further oxidized by $\text{SO}_4^{\cdot-}$ and HO^\cdot to form ClO_3^- (Lutze et al., 2015). In the UV/PMS system, ClO_3^- formation was significantly slow as compared with that in UV/PDS (**Figure 8**). It might be due to the reaction between $\text{Cl}^\cdot/\text{Cl}_2^{\cdot-}$ and PMS (Guan et al., 2018), which resulted in the reduction of $\text{Cl}^\cdot/\text{Cl}_2^{\cdot-}$ into Cl^- by PMS (Reactions 20 and 21) and therefore prevented the formation of Cl_2 from $\text{Cl}^\cdot/\text{Cl}_2^{\cdot-}$ recombination, cutting down the pathway of ClO_3^- formation from $\text{Cl}^\cdot/\text{Cl}_2^{\cdot-}$ recombination. However, Cl^- could be oxidized by PMS directly via Reactions 22 and 23 although with a low rate constant (Lente et al., 2009; Zhou et al., 2018). This would be the origin of slow chlorate formation in UV/PMS. In UV/ H_2O_2 , $\text{Cl}^\cdot/\text{Cl}_2^{\cdot-}$ might be formed via Reactions 24–26. Meanwhile, $\text{Cl}^\cdot/\text{Cl}_2^{\cdot-}$ reacts fast with H_2O_2 and would be reduced readily to Cl^- via Reactions 27 and 28 (Guan et al., 2018). Furthermore, $\text{HOCl}/\text{ClO}^\cdot$ could be reduced by H_2O_2 (Held et al., 1978) even if it was formed from $\text{Cl}^\cdot/\text{Cl}_2^{\cdot-}$ radical combination, which resulted in the phenomenon that no ClO_3^- was formed in UV/ H_2O_2 as shown in **Figure 8**.



In tap water, no BrO_3^- or ClO_3^- was detected with added Br^- initial concentration of $10 \mu\text{M}$ or Cl^- initial concentration of 0.5 mM in all three oxidation systems. Water quality parameters are listed in **Table 5**. NOM in tap water competed for HO^\cdot and $\text{SO}_4^{\cdot-}$ with the rate constants of $1.4 \times 10^4 (\text{mgTOC L}^{-1})^{-1} \text{ s}^{-1}$ and $2.2 \times 10^3 (\text{mgTOC L}^{-1})^{-1} \text{ s}^{-1}$ (Guan et al., 2018). Based on the competition kinetics, NOM and bicarbonate would compete for part of HO^\cdot and $\text{SO}_4^{\cdot-}$ with $10 \mu\text{M}$ Br^- and very limited quantity of HO^\cdot and $\text{SO}_4^{\cdot-}$ with 0.5 mM Cl^- . $\text{Br}^\cdot/\text{Br}_2^{\cdot-}$

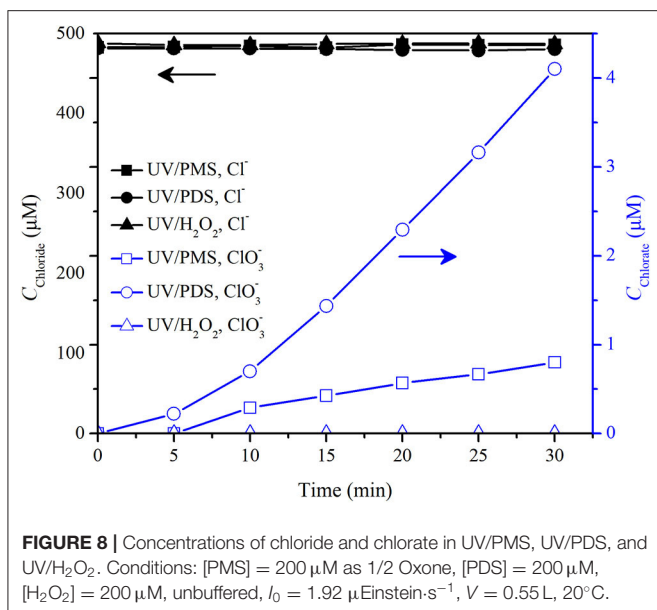


FIGURE 8 | Concentrations of chloride and chlorate in UV/PMS, UV/PDS, and UV/H₂O₂. Conditions: [PMS] = 200 μM as 1/2 Oxone, [PDS] = 200 μM, [H₂O₂] = 200 μM, unbuffered, $I_0 = 1.92 \mu\text{Einstein}\cdot\text{s}^{-1}$, $V = 0.55 \text{ L}$, 20°C.

and $\text{Cl}^-/\text{Cl}_2^-$ would form. It was reported that Cl^- turned SO_4^- into $\text{HO}\cdot$ at pH 7 in UV/PDS (Lutze et al., 2015) and increasing pH also increased the conversion of SO_4^- to $\text{HO}\cdot$ and lowered the conversion of SO_4^- to $\text{Cl}^-/\text{Cl}_2^-$ in UV/PMS (Guan et al., 2018). The neutral pH condition would not favor the formation of $\text{Br}^-/\text{Br}_2^-$ and $\text{Cl}^-/\text{Cl}_2^-$ and subsequent formation of BrO_3^- and ClO_3^- in UV/PDS and UV/PMS in tap water at pH 6.98. Meanwhile, NOM and HCO_3^- could react with $\text{Br}^-/\text{Br}_2^-$ or $\text{Cl}^-/\text{Cl}_2^-$ and would prevent the formation of $\text{HOBr}/\text{BrO}^-/\text{Br}_2/\text{Br}_3^-$ or $\text{HOCl}/\text{ClO}^-/\text{Cl}_2$ from Br^- and Cl^- by radical oxidation, cutting down the formation of BrO_3^- and ClO_3^- from the pathway of $\text{Br}^- \rightarrow \text{Br}^-/\text{Br}_2^- \rightarrow \text{HOBr}/\text{BrO}^-/\text{Br}_2/\text{Br}_3^- \rightarrow \text{BrO}_3^-$ and $\text{Cl}^- \rightarrow \text{Cl}^-/\text{Cl}_2^- \rightarrow \text{HOCl}/\text{ClO}^-/\text{Cl}_2 \rightarrow \text{ClO}_3^-$. Although Br^- and Cl^- might be oxidized directly to $\text{HOBr}/\text{BrO}^-/\text{Br}_2/\text{Br}_3^-$ or $\text{HOCl}/\text{ClO}^-/\text{Cl}_2$ via two-electron transfer by PMS (Lente et al., 2009; Zhou et al., 2018), NOM and bicarbonate in tap water would compete for most of SO_4^- , $\text{HO}\cdot$, $\text{Br}^-/\text{Br}_2^-$, or $\text{Cl}^-/\text{Cl}_2^-$ with $\text{BrO}_3^-/\text{ClO}_3^-$ intermediates formed in low concentration (such as HOBr/BrO^- or HOCl/ClO^-), hindering the formation of BrO_3^- and ClO_3^- .

CONCLUSIONS

Oxidation of different reactivity compounds and formation of bromate and chlorate were investigated in UV/peroxide processes (UV/PMS, UV/PDS, and UV/H₂O₂), as well as inhibition of inorganic and organic carbon on the three processes. NOM showed the largest inhibition on the UV/H₂O₂ process and smallest on the UV/PDS process due to the smaller ratio of rate constants of $\text{HO}\cdot$ with BA and NOM than SO_4^- , while HCO_3^- and CO_3^{2-} exhibited largest inhibition on the UV/PDS process. Furthermore, the inhibition of CO_3^{2-} was more significant than HCO_3^- on all three UV/peroxide processes. The difference of inhibition extent of CO_3^{2-} on the UV/peroxides

was smaller than HCO_3^- . This was ascribed to the conversion of SO_4^- to $\text{HO}\cdot$ under alkaline conditions (pH 11) and the high rate constant between $\text{HO}\cdot$ and CO_3^{2-} .

UV/H₂O₂ showed higher decontamination efficiencies than UV/PDS and UV/PMS for BA degradation under acidic and neutral conditions, while UV/PMS showed outstanding decontamination efficiency for BA degradation under alkaline conditions. The performance of UV/peroxide processes declined in the sequence of UV/H₂O₂ > UV/PMS > UV/PDS for NB degradation under acidic and neutral conditions. Meanwhile, UV/PMS also showed excellent decontamination efficiency for NB degradation under alkaline conditions. UV/peroxide performance for TCM degradation was in the increased sequence of UV/H₂O₂ < UV/PMS < UV/PDS under all pH conditions. The high removal efficiencies for TCM by UV/PDS, as compared with the other two UV/peroxide processes, might be due to the lower scavenging of radicals (SO_4^- , $\text{HO}\cdot$, and Cl^-) by the parent oxidant (PDS) in the reaction system.

In pure water background, 7.8 μM BrO_3^- was formed by 30 min at an initial Br^- concentration of 9.8 μM and an oxidant concentration of 200 μM in UV/PDS, while 2.4 μM BrO_3^- was formed in UV/PMS and no BrO_3^- was detected in UV/H₂O₂. 4 μM ClO_3^- was formed by 30 min in pure water at an initial Cl^- concentration of 0.5 mM and an oxidant concentration of 200 μM in UV/PDS. 0.8 μM ClO_3^- was formed by 30 min in UV/PMS and no ClO_3^- was detected in UV/H₂O₂. In tap water, no BrO_3^- or ClO_3^- was detected with added Br^- initial concentration of 10 μM or Cl^- initial concentration of 0.5 mM in all three oxidation processes.

Based on the comparison of UV/peroxide processes, it was suggested that UV/PMS would be used in alkaline water bodies and UV/H₂O₂ would be suitable under acidic and neutral conditions for destructing organic pollutants with high rate constants toward radicals, while UV/PDS might be efficient for removing chloro-substituted organic compounds with low rate constants toward radicals, but need serious concern on controlling the oxidation time to avoid chlorate formation via over-oxidation.

DATA AVAILABILITY STATEMENT

The raw data supporting the conclusions of this article will be made available by the authors, without undue reservation.

AUTHOR CONTRIBUTIONS

Y-HG: responsible for manuscript writing, experiment design, and data analysis. JC: experiment conduction and data analysis. L-JC and X-XJ: data analysis and validation. QF: supervision, validation, and funding acquisition. All authors contributed to the article and approved the submitted version.

FUNDING

This work was supported by the National Natural Science Foundation of China (Grant Nos. 51408107 and 41701102), the

National Science Fund for Distinguished Young Scholars (Grant No. 51825901), the University Nursing Program for Young Scholars with Creative Talents in Heilongjiang province (Grant No. UNPYSCT-2018166), the Natural Science Foundation

of Heilongjiang Province (Grant No. LH2019E013), the Heilongjiang postdoctoral Fund (Grant No. LBH-Q19072), and the Young Talents Project of Northeast Agricultural University (Grant No. 17QC09).

REFERENCES

- Anipsitakis, G. P., and Dionysiou, D. D. (2004). Transition metal/UV-based advanced oxidation technologies for water decontamination. *Appl. Catal. B Environ.* 54, 155–163. doi: 10.1016/j.apcatb.2004.05.025
- Bader, H., Sturzenegger, V., and Hoigné, J. (1988). Photometric method for the determination of low concentrations of hydrogen peroxide by the peroxidase catalyzed oxidation of N,N-diethyl-p-phenylenediamine (DPD). *Water Res.* 22, 1109–1115. doi: 10.1016/0043-1354(88)90005-X
- Ball, R. E., Edwards, J. O., Hagggett, M. L., and Jones, P. (1967). A kinetic and isotopic study of the decomposition of monoperoxyphthalic acid. *J. Am. Chem. Soc.* 89, 2331–2333. doi: 10.1021/ja00986a015
- Baxendale, J. H., and Wilson, J. A. (1957). The photolysis of hydrogen peroxide at high light intensities. *Trans. Faraday Soc.* 53, 344–356. doi: 10.1039/tf9575300344
- Bennedsen, L. R., Muffa, J., and Søgaard, E. G. (2012). Influence of chloride and carbonates on the reactivity of activated persulfate. *Chemosphere* 86, 1092–1097. doi: 10.1016/j.chemosphere.2011.12.011
- Chi, H. Z., He, X., Zhang, J. Q., and Jun Ma, J. (2019). Efficient degradation of refractory Organic contaminants by zero-valent copper/hydroxylamine/peroxymonosulfate process. *Chemosphere* 237:124431. doi: 10.1016/j.chemosphere.2019.124431
- Cong, J., Wen, G., Huang, T. L., Deng, L. Y., and Ma, J. (2015). Study on enhanced ozonation degradation of para-chlorobenzoic acid by peroxymonosulfate in aqueous solution. *Chem. Eng. J.* 264, 399–403. doi: 10.1016/j.cej.2014.11.086
- Crittenden, J. C., Hu, S., Hand, D. W., and Green, S. A. (1999). A kinetic model for H₂O₂/UV process in a completely mixed batch reactor. *Water Res.* 33, 2315–2328. doi: 10.1016/S0043-1354(98)00448-5
- Ding, J., Bu, L. J., Zhao, Q. L., Kabutey, F. T., Wei, L. L., Dionysiou, D. D., et al. (2020). Electrochemical activation of persulfate on Bdd and Dsa anodes: electrolyte influence, kinetics and mechanisms in the degradation of bisphenol A. *J. Hazard Mater.* 388:121789. doi: 10.1016/j.jhazmat.2019.121789
- Ebersson, L. (1982). Electron-transfer reactions in organic chemistry. *Adv. Phys. Org. Chem.* 18, 79–185. doi: 10.1016/S0065-3160(08)60139-2
- Fang, J. Y., and Shang, C. (2012). Bromate formation from bromide oxidation by the UV/persulfate process. *Environ. Sci. Technol.* 46, 8976–8983. doi: 10.1021/es300658u
- Furman, O. S., Teel, A. L., and Watts, R. J. (2010). Mechanism of base activation of persulfate. *Environ. Sci. Technol.* 44, 6423–6428. doi: 10.1021/es1013714
- Guan, Y. H., Ma, J., Li, X. C., Fang, J. Y., and Chen, L. W. (2011). Influence of pH on the formation of sulfate and hydroxyl radicals in the UV/peroxymonosulfate system. *Environ. Sci. Technol.* 45, 9308–9314. doi: 10.1021/es2017363
- Guan, Y. H., Ma, J., Liu, D. K., Ou, F. Z., Zhang, W. Q., Gong, X. L., et al. (2018). Insight into chloride effect on the UV/peroxymonosulfate process. *Chem. Eng. J.* 352, 477–489. doi: 10.1016/j.cej.2018.07.027
- Guan, Y. H., Ma, J., Ren, Y. M., Liu, Y. L., Xiao, J. Y., Lin, L. Q., et al. (2013). Efficient degradation of atrazine by magnetic porous copper ferrite catalyzed peroxymonosulfate oxidation via the formation of hydroxyl and sulfate radicals. *Water Res.* 47, 5431–5438. doi: 10.1016/j.watres.2013.06.023
- He, X., de la Cruz, A. A., and Dionysiou, D. D. (2013). Destruction of cyanobacterial toxin cylindrospermopsin by hydroxyl radicals and sulfate radicals using UV-254nm activation of hydrogen peroxide, persulfate and peroxymonosulfate. *J. Photochem. Photobiol. A Chem.* 251, 160–166. doi: 10.1016/j.jphotochem.2012.09.017
- He, X. X., Mezyk, S. P., Michael, I., Fatta-Kassinos, D., and Dionysiou, D. D. (2014). Degradation kinetics and mechanism of beta-lactam antibiotics by the activation of H₂O₂ and Na₂S₂O₈ under UV-254nm irradiation. *J. Hazard Mater.* 279, 375–383. doi: 10.1016/j.jhazmat.2014.07.008
- Heidt, L. J., Mann, J. B., and Schneider, H. R. (1948). The photolysis of persulfate. II. The quantum yield in water and the effect of sodium chloride in dilute alkaline solution. *J. Am. Chem. Soc.* 70, 3011–3015. doi: 10.1021/ja01189a052
- Held, A. M., Halko, D. J., and Hurst, J. K. (1978). Mechanisms of chlorine oxidation of hydrogen peroxide. *J. Am. Chem. Soc.* 100, 5732–5740. doi: 10.1021/ja00486a025
- Hou, S., Ling, L., Dionysiou, D. D., Wang, Y., Huang, J., Guo, K., et al. (2018). Chlorate formation mechanism in the presence of sulfate radical, chloride, bromide and natural organic matter. *Environ. Sci. Technol.* 52, 6317–6325. doi: 10.1021/acs.est.8b00576
- Hu, J. M., Zhang, J., Wang, Q. G., Ye, Q., Xu, H., Zhou, G. Y., et al. (2019). Efficient degradation of tetracycline by ultraviolet-based activation of peroxymonosulfate and persulfate. *Water Sci. Technol.* 79, 911–920. doi: 10.2166/wst.2019.034
- Koppenol, W. H., and Butler, J. (1985). Energetics of interconversion reactions of oxyradicals. *Free Radical Bio. Med.* 1, 91–131. doi: 10.1016/8755-9668(85)90005-5
- Lente, G., Kalmár, J., Baranyai, Z., Kun, A., Kék, I., Bajusz, D., et al. (2009). One- versus Two-electron oxidation with peroxomonosulfate ion: reactions with Iron(II), Vanadium(IV), halide ions, and photoreaction with Cerium(III). *Inorg. Chem.* 48, 1763–1773. doi: 10.1021/ic801569k
- Li, Z. Y., Wang, L., Liu, Y. L., Zhao, Q., and Ma, J. (2020). Unraveling the interaction of hydroxylamine and Fe(III) in Fe(II)/persulfate system: a kinetic and simulating study. *Water Res.* 168:115093. doi: 10.1016/j.watres.2019.115093
- Liu, X., Yuan, B. L., Zou, J., Wu, L. B., Dai, L., Ma, H. F., et al. (2020). Cu(II)-enhanced degradation of acid orange 7 by Fe(II)-activated persulfate with hydroxylamine over a wide pH range. *Chemosphere* 238:124533. doi: 10.1016/j.chemosphere.2019.124533
- Liu, Y., Yang, Y., Pang, S., Zhang, L., Ma, J., Luo, C., et al. (2018). Mechanistic insight into suppression of bromate formation by dissolved organic matters in sulfate radical-based advanced oxidation processes. *Chem. Eng. J.* 333, 200–205. doi: 10.1016/j.cej.2017.09.159
- Luo, C. W., Gao, J., Ma, Q., Wu, D., Cheng, X., Jiang, J., et al. (2020). The bromate formation accompanied by the degradation of 2,4-bromophenol in UV/peroxymonosulfate. *Sep. Purif. Technol.* 233:116028. doi: 10.1016/j.seppur.2019.116028
- Luo, C. W., Gao, J., Wu, D. J., Jiang, J., Liu, Y. Z., Zhou, W. W., et al. (2019). Oxidation of 2,4-bromophenol by UV/PDS and formation of bromate and brominated products: a comparison to UV/H₂O₂. *Chem. Eng. J.* 358, 1342–1350. doi: 10.1016/j.cej.2018.10.084
- Luo, C. W., Ma, J., Jiang, J., Liu, Y. Z., Song, Y., Yang, Y., et al. (2015). Simulation and comparative study on the oxidation kinetics of atrazine by UV/H₂O₂, UV/HSO₅⁻ and UV/S₂O₈²⁻. *Water Res.* 80, 99–108. doi: 10.1016/j.watres.2015.05.019
- Lutze, H. V., Kerlin, N., and Schmidt, T. C. (2015). Sulfate radical-based water treatment in presence of chloride: formation of chlorate, inter-conversion of sulfate radicals into hydroxyl radicals and influence of bicarbonate. *Water Res.* 72, 349–360. doi: 10.1016/j.watres.2014.10.006
- Neta, P., Huie, R. E., and Ross, A. B. (1988). Rate constants for reactions of inorganic radicals in aqueous solution. *J Phys Chem. Ref. Data.* 17, 1027–1284. doi: 10.1063/1.555808
- Qian, Y., Guo, X., Zhang, Y., Peng, Y., Sun, P., Huang, C. H., et al. (2016). Perfluorooctanoic acid degradation using UV-persulfate process: Modeling of the degradation and chlorate formation. *Environ. Sci. Technol.* 50, 772–781. doi: 10.1021/acs.est.5b03715
- Rayaroth, M. P., Lee, C. S., Aravind, U. K., Aravindakumar, C. T., and Chang, Y. S. (2017). Oxidative degradation of benzoic acid using Fe⁰ - and sulfidized Fe⁰ - activated persulfate: a comparative study. *Chem. Eng. J.* 315, 426–436. doi: 10.1016/j.cej.2017.01.031

- Sun, Y. Q., Cho, D. W., Graham, N. J. D., Hou, D., Yip, A. C. K., Khan, E., et al. (2019). Degradation of antibiotics by modified vacuum-UV based processes: mechanistic consequences of H₂O₂ and K₂S₂O₈ in the presence of halide ions. *Sci. Total. Environ.* 664, 312–321. doi: 10.1016/j.scitotenv.2019.02.006
- Von Gunten, U., and Oliveras, Y. (1997). Kinetics of the reaction between hydrogen peroxide and hypobromous acid: implication on water treatment and natural systems. *Water Res.* 31, 900–906. doi: 10.1016/S0043-1354(96)00368-5
- von Gunten, V. U., and Oliveras, Y. (1998). Advanced oxidation of bromide-containing waters: bromate formation mechanisms. *Environ. Sci. Technol.* 32, 63–70. doi: 10.1021/es970477j
- Wang, Q. F., Rao, P. H., Li, G. H., Dong, L., Zhang, X., Shao, Y. S., et al. (2020). Degradation of imidacloprid by UV-activated persulfate and peroxymonosulfate processes: kinetics, impact of key factors and degradation pathway. *Ecotoxicol. Environ. Saf.* 187:109779. doi: 10.1016/j.ecoenv.2019.109779
- Wang, Z. Y., An, N., Shao, Y. S., Gao, N. Y., Du, E. D., Xu, B., et al. (2020). Experimental and simulation investigations of UV/persulfate treatment in presence of bromide: effects on degradation kinetics, formation of brominated disinfection byproducts and bromate. *Sep. Purif. Technol.* 242:116767. doi: 10.1016/j.seppur.2020.116767
- Wei, T., Waqas, M., Xiao, K., Yang, B., Luo, Y., Luo, Q. H., et al. (2019). Effective degradation of refractory nitrobenzene in water by the natural 4-hydroxycoumarin under solar illumination. *Chemosphere* 215, 199–205. doi: 10.1016/j.chemosphere.2018.10.034
- Xiao, R. Y., He, L., Luo, Z. H., Spinney, R., Wei, Z. S., Dionysiou, D. D., et al. (2020b). An experimental and theoretical study on the degradation of clonidine by hydroxyl and sulfate radicals. *Sci. Total. Environ.* 710:136333. doi: 10.1016/j.scitotenv.2019.136333
- Xiao, R. Y., Ma, J. Y., Luo, Z. H., Wei, Z. S., Spinney, R., Hu, W. P., et al. (2020a). Experimental and theoretical insight into hydroxyl and sulfate radicals-mediated degradation of carbamazepine. *Environ. Pollut.* 257:113498. doi: 10.1016/j.envpol.2019.113498
- Xie, P., Ma, J., Liu, W., Zou, J., Yue, S., Li, X., et al. (2015). Removal of 2-MIB and geosmin using UV/persulfate: contributions of hydroxyl and sulfate radicals. *Water Res.* 69, 223–233. doi: 10.1016/j.watres.2014.11.029
- Yang, Z. H., Su, R. K., Luo, S., Spinney, R., Cai, M. Q., Xiao, R. Y., et al. (2017). Comparison of the reactivity of ibuprofen with sulfate and hydroxyl radicals: an experimental and theoretical study. *Sci. Total. Environ.* 590–591, 751–760. doi: 10.1016/j.scitotenv.2017.03.039
- Zhang, W., Zhou, S., Sun, J., Meng, X., Luo, J., Zhou, D., et al. (2018). Impact of chloride ions on UV/H₂O₂ and UV/persulfate advanced oxidation processes. *Environ. Sci. Technol.* 52, 7380–7389. doi: 10.1021/acs.est.8b01662
- Zhou, Y., Jiang, J., Gao, Y., Pang, S. Y., Ma, J., Duan, J., et al. (2018). Oxidation of steroid estrogens by peroxymonosulfate (PMS) and effect of bromide and chloride ions: kinetics, products, and modeling. *Water Res.* 138, 56–66. doi: 10.1016/j.watres.2018.03.045
- Zrinyi, N., and Pham, A. L. T. (2017). Oxidation of benzoic acid by heat-activated persulfate: effect of temperature on transformation pathway and product distribution. *Water Res.* 120, 43–51. doi: 10.1016/j.watres.2017.04.066

Conflict of Interest: The authors declare that the research was conducted in the absence of any commercial or financial relationships that could be construed as a potential conflict of interest.

Copyright © 2020 Guan, Chen, Chen, Jiang and Fu. This is an open-access article distributed under the terms of the Creative Commons Attribution License (CC BY). The use, distribution or reproduction in other forums is permitted, provided the original author(s) and the copyright owner(s) are credited and that the original publication in this journal is cited, in accordance with accepted academic practice. No use, distribution or reproduction is permitted which does not comply with these terms.